DE GRUYTER

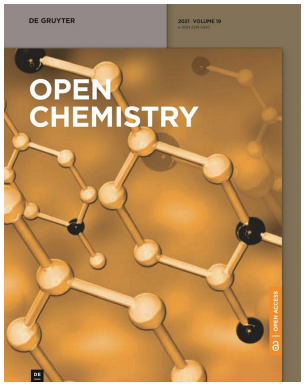

Impact Factor: 1.977

Open Access | Published since March 1, 2003

Open Chemistry

ISSN: 2391-5420

Submit manuscript

Editorial

Editors

Publisher

DE GRUYTER Poland
Bogumiła Zuga 32A Str.
01-811 Warsaw, Poland
T: +48 22 701 50 15

Editorial Contact
openchemistry@degruyter.com

Assistant Managing Editor
Kumaran Rengaswamy
Assistant Managing Editor, Compuscript
AssistantManagingEditor@degruyter.com

Type: Journal
Language: English
Publisher: De Gruyter Open Access
First published: March 1, 2003
Publication Frequency: 1 Issue per Year

DE GRUYTER

Open Access | Published by De Gruyter Open Access

Volume 17 Issue 1

January 2019

Issue of Open Chemistry

Submit manuscript

CONTENTS JOURNAL OVERVIEW

Regular Articles

Open Access | January 8, 2019

Research on correlation of compositions with oestrogenic activity of *Cistanche* based on LC/Q-TOF-MS/MS technology

Wen-Lan Li, Jing-Xin Ding, Jing Bai, Yang Hu, Hui Song, Xiang-Ming Sun, Yu-Bin Ji

Page range: 1-12

Abstract

LC technology is a recognized method used worldwide to evaluate the quality of traditional Chinese medicines (TCM). The quality of TCM has a direct impact on its efficacy. Therefore, in order to thoroughly reveal how TCM exerts its efficacy, first of all, it is necessary to understand the material basis for its efficacy, and then to control the quality of active compounds. The application of the spectrum-effect relationship method is crucial for determining the pharmacological material basis. The goal of this paper was to investigate the underlying correlations between the chemical profiles and oestrogenic activity of Cistanche , to reveal the active compounds. The chemical profiles of Cistanche were recorded using HPLC/Q-TOF-MS/MS, and oestrogenic activity was determined by the Uterus growth test and the MTT assay. Then combining the results of bivariate analysis, principal component analysis and gray correlation analysis method, fifteen active compounds were identified. They are 8-epiloganic acid, salidroside, syringalide A 3'-α-l-rhamnopyranoside, cistanoside A, echinacoside, cistanoside F, cistanoside B,

retained SOCs with specific qualities in relation to their functional microorganisms should be further explored in the future.

Open Access | December 31, 2019

A potential reusable fluorescent aptasensor based on magnetic nanoparticles for ochratoxin A analysis

Pinzhu Qin, Dawei Huang, Zihao Xu, Ying Guan, Yongxin Bing, Ang Yu

Page range: 1301–1308

Abstract

An aptasensor for the detection of ochratoxin A (OTA) in environmental samples was developed. It displayed high sensitivity and good selectivity. Factors such as specific binding between a FAM (5-carboxyfluorescein)-labeled aptamer (f-RP) and OTA, and a magnetic property of a streptavidin magbeads-modified capture probe (bm-CP) resulted in aptasensor's linear relationship between fluorescence intensity and the concentration of OTA. This characteristic is present at the OTA concentration ranges from 0.100 μM to 25.00 μM with a LOD (limit of detection) of 0.0690 μM. The bm-CP can be reused through melting, washing and magnetic separation, which contributes to cost reduction. In addition, the proposed method is simple and detection process is fast. The aptasensor can be used in real samples.

Special Issue on 13th JCC 2018

Open Access | August 24, 2019

Fluorescence study of 5-nitroisatin Schiff base immobilized on SBA-15 for sensing Fe^{3+}

Muhammad Riza Ghulam Fahmi, Adroit T.N. Fajar, Nurliana Roslan, Leny Yuliati, Arif Fadlan, Mardi Santoso, Hendrik O. Lintang

Page range: 438–447

Abstract

N '-(5-nitro-2-oxoindolin-3-ylidene) thiophene-2-carbohydrazide (NH) was successfully synthesized as a ligand, then grafted onto the surface of mesoporous silica SBA-15 via an aminopropyl bridge. The successful grafting of ligand NH onto the hybrid nanomaterial (SBA-15/APTES-NH) was confirmed by infrared spectroscopy. On excitation at 276 and 370 nm, the ligand NH and the hybrid nanomaterial SBA-15/APTES-NH showed a strong and narrow emission peak centered at 533 nm. By dispersing SBA-15/APTES-NH in an aqueous solution containing metal ions, the resulting solid

materials showed a higher binding of NH sensing site to Fe 3+ ions as compared to the others with a quench of the emission intensity up to 84%. This result showed that the hybrid nanomaterial is a potential chemosensor that requires development for the detection of metal ions.

Open Access | August 12, 2019

Thermal and Morphology Properties of Cellulose Nanofiber from TEMPO-oxidized Lower part of Empty Fruit Bunches (LEFB)

Mahendra I.P., Wirjosentono B., Tamrin, Ismail H., Mendez J.A.

Page range: 526-536

Abstract

Cellulose nanofiber (CNF) gel has been obtained from TEMPO-oxidized differently treated lower part of empty fruit bunches (LEFB) of oil palm. Three kinds of materials were initially used: (i) α-cellulose, (ii) raw LEFB fiber two-times bleaching, and (iii) raw LEFB three-times bleaching. The obtained nanofibers (CNF1, CNF2 and CNF3, respectively) were then characterized using several methods, e.g. FT-IR, SEM, UV-Visible, TEM, XRD and TGA. The LEFB at different levels of bleaching showed that the Kappa number decreased with the increase of the bleaching levels. The decrease of lignin and hemicellulose content affected the increase of the yield of fibrillation and optical transmittance of CNF2 and CNF3 gels. The FT-IR analysis confirmed the presence of lignin and hemicellulose in the CNF2 and CNF3 film. Based on TEM analysis, the lignin and hemicellulose content significantly affected the particle structure of CNFs, i.e . CNF1 was found as a bundle of fibril, while the CNF2 and CNF3 were visualized as individual fibers and interwoven nanofibril overlapping each other, respectively. The XRD data of the CNF's film showed that CNF2 and CNF3 have a lower crystallinity index (CI) than CNF1. The presence of lignin and hemicellulose in the CNFs decreased its decomposition temperature.

Open Access | August 24, 2019

Encapsulation of Vitamin C in Sesame Liposomes: Computational and Experimental Studies

Dwi Hudiyanti, Noor Ichsan Hamidi, Daru Seto Bagus Anugrah, Siti Nur Milatus Salimah, Parsaoran Siahaan

Page range: 537-543

Abstract

An experimental and computational study was carried out for encapsulation of vitamin C in sesame, Sesamum indicum L., liposomes. Based on

computational studies, the packing parameter (P) of sesame phospholipids was found to be 0.64 ± 0.09. This indicates that the molecular shape of sesame phospholipids is in the form of truncated cone and, in aqueous solution, it self-assembles to form liposomes. In the liposomes, no chemical interaction was observed between phospholipid molecules and vitamin C. However, medium-strength hydrogen bonds (E i) from -87.6 kJ/mol to -82.02 kJ/mol with bond lengths ranging from 1.746 Å to 1.827 Å were formed between vitamin C and phospholipid molecules. Because of this weak interaction, vitamin C gets released easily from the inner regions of liposome. Empirical experiments were performed to confirm the computation outcomes, where sesame liposomes were found to encapsulate almost 80% of vitamin C in their interior cavities. During the 8 days storage, release of vitamin C occurred gradually from the liposome system, which signifies week interactions in the liposome membranes amongst phospholipid molecules and vitamin C.

Open Access | August 19, 2019

A comparative study of the utilization of synthetic foaming agent and aluminum powder as pore-forming agents in lightweight geopolymer synthesis

Ufafa Anggarini, Suminar Pratapa, Victor Purnomo, Ndaru Candra Sukmana

Page range: 629–638

Abstract

Lightweight geopolymer concrete was synthesized using fly ash as an aluminosilicate source with the addition of a pore-forming agent. The synthesis of a geopolymer was conducted by employing various volume ratios of geopolymer paste to the foaming agent: 1:0.50, 1:0.67, 1:0.75, 1:1.00, 1:1.33, 1:1.50, and 1:2.00, while the ratios of aluminum powder weight percentage to the fly ash weight varied between 0.01 - 0.15 %wt. The results showed that the higher foaming agent content, the lower the compressive strength and density of the geopolymer. The ratio of the geopolymer paste to the foaming agent, 1:1.33 was found to produce the strongest light weight geopolymer whose compressive strength and density were 33 MPa and 1760 kg/m 3 , respectively. With the addition of 0.01%wt aluminum powder, the geopolymer specimen showed the highest compressive strength of 42 MPa and density of 1830 kg/m 3 , respectively. X-Ray Diffraction (XRD), Scanning Electron Microscope (SEM) and FT-IR were utilized to study the effects of foaming agent and aluminum powder addition onto the microstructure, surface morphology, and functional groups of the geopolymer. Both types of synthesized geopolymers have the potential to be developed in terms of compressive strength and density in the future.

Open Access | December 31, 2019

Synthesis of high surface area mesoporous silica SBA-15 by adjusting hydrothermal treatment time and the amount of polyvinyl alcohol

Ridhawati Thahir, Abdul Wahid Wahab, Nursiah La Nafie, Indah Raya

Page range: 963-971

Abstract

The high surface area of mesoporous silica SBA-15 has been synthesized successfully by hydrothermal treatment with direct addition of PVA, triblock copolymer (P123) as a direct structure agent and tetraethyl orthosilicate (TEOS) as a precursor. The mesoporous silica SBA-15 have been characterized with nitrogen physisorption, scanning electron microscopy, Fourier transformed infrared spectroscopy, and x-ray diffraction. Measurement of nitrogen sorption indicated that with the addition of PVA, the surface area is increased but the pore volume and pore diameter is not significantly. The short time of hydrothermal treatment (20 h) and using x-ray diffraction, showed that the morphological structure of silica SBA-15 can be changed to a orthorhombic crystal system. The result of the FTIR and SEM-EDX characteristic indicated the functional groups and morphology of the SBA-15

with a narrow pore size distribution. The BET method has exhibited the largest surface area 1726 m 2 /g, pore volume 1.4 cm 3 /g, and pore diameter 3.2 nm. It can be suggested that the silica mesoporous SBA-15 will have potential application prospect in catalysis, storage, and adsorbent.

Open Access | November 13, 2019

Review of large-pore mesostructured cellular foam (MCF) silica and its applications

Lilis Hermida, Joni Agustian, Ahmad Zuhairi Abdullah, Abdul Rahman Mohamed

Page range: 1000–1016

Abstract

The unique properties of mesostructured cellular foam (MCF) silica such as, large pore size, continuous three-dimensional (3D) pore system and hydrothermal robust materialallow favorable conditions for incorporating active sites to produce modified MCF silica as catalysts, biocatalysts and adsorbents. Recently, the modified MCF silicas were reported to be efficient catalysts for the hydrogenation of phenylacetylene, heck coupling reaction of arylboronic acid, etc. Biocatalysts derived from modified MCF silicas were found to be a potential to convert glucose to gluconic acid, hydrolysis of N-benzoyl-DLarginine-p-nitroanilide (BAPNA) and casein, transesterification of racemic 1 phenyl- ethanol and hydrolytic, etc. Several separation processes such as CO 2 capture and adsorption of L-tryptophan, lysozyme and bovine serum were sucessfully conducted using adsorbents derived from modified MCF silicas. This paper reviews the synthesis of the MCF silica material and the incorporation of active sites or immobilization of enzymes in the MCF silica material. Additionally, a detailed understanding of the characterization of the modified MCF silicas, which includes pore size, active sites/enzymes sizes, amount of active sites/enzymes bound with the MCF silica, was also discussed to obtain their potentialities as catalysts, biocatalysts and adsorbents. The review also describes recent progress on the applications of the MCF silica.

Open Access | November 13, 2019

Ion Exchange of Benzoate in Ni-Al-Benzoate Layered Double Hydroxide by Amoxicillin

Dian Windy Dwiasi, Mudasir Mudasir, Roto Roto

Page range: 1043–1049

Research Article

Ridhawati Thahir*, Abdul Wahid Wahab, Nursiah La Nafie, Indah Raya

Synthesis of high surface area mesoporous silica SBA-15 by adjusting hydrothermal treatment time and the amount of polyvinyl alcohol

https://doi.org/10.1515/chem-2019-0106
received September 18, 2018; accepted May 16, 2019.

Abstract: The high surface area of mesoporous silica SBA-15 has been synthesized successfully by hydrothermal treatment with direct addition of PVA, triblock copolymer (P123) as a direct structure agent and tetraethyl orthosilicate (TEOS) as a precursor. The mesoporous silica SBA-15 have been characterized with nitrogen physisorption, scanning electron microscopy, Fourier transformed infrared spectroscopy, and x-ray diffraction. Measurement of nitrogen sorption indicated that with the addition of PVA, the surface area is increased but the pore volume and pore diameter is not significantly. The short time of hydrothermal treatment (20 h) and using x-ray diffraction, showed that the morphological structure of silica SBA-15 can be changed to a orthorhombic crystal system. The result of the FTIR and SEM-EDX characteristic indicated the functional groups and morphology of the SBA-15 with a narrow pore size distribution. The BET method has exhibited the largest surface area 1726 m^2/g, pore volume 1.4 cm^3/g, and pore diameter 3.2 nm. It can be suggested that the silica mesoporous SBA-15 will have potential application prospect in catalysis, storage, and adsorbent.

Keywords: mesoporous silica; SBA-15; surface area; hydrothermal treatment.

***Corresponding author: Ridhawati Thahir,** Chemical Engineering Department, State Polytechnic of Ujung Pandang, Jl. Perintis Kemerdekaan Km. 10 Makassar, Indonesia, E-mail: ridha331@poliupg.ac.id
Abdul Wahid Wahab, Nursiah La Nafie, Indah Raya, Department of Chemistry, Faculty of Mathematics and Natural Science, Hasanuddin University, Makassar, Indonesia

1 Introduction

Porous materials are established as a solid have content of pores and the fraction of pore volume to the total volume 0.2-0.95 [1]. According to the IUPAC, porous materials have a classified base on pore size. They are macropores (pore diameter with more than 50 nm); mesopores (pore diameter between 2 nm and 50 nm) and micropores (pores with diameter no more than 2 nm) [2]. Santa Barbara Amorphous (SBA-15) is one of the typical mesoporous bases on silica that has well ordered hexagonal structure with uniform pore size up to 30 nm [3].

Previous studies have reported that mesoporous silica SBA-15 had advanced structure properties, such as high specific surface area to acquire many active sites in insufficient volume [4], uniformity of pore diameter to permit diffusion and adsorption of larger molecules [5–8], thick pore wall and exceptionally hydrothermal stability [9], and specify structure is still a considerable role for future material scientist [10]. The excellent mesoporous materials of SBA-15 can be used in an amount of application such as catalysis [11–13], water treatment [14,15], sensor [16–18], and supporting cell for composite materials [12,18–20]. The mesoporous materials, high surface area, and high thermal stability have widely used for more application in industry. In spite of properties of the SBA-15 in various application, it is still required to modify variable synthesis of SBA-15.

The changes experienced by the enhanced high surface area of SBA-15 had been studied by many researchers using the addition of PVA (polyvinyl alcohol). It was investigated that the surface area of SBA-15 is increased to 1248 m^2/g while the structure and pore size stable [4]. This concept has recently been challenged by a decreased surface area of SBA-15, their studies explaining that added PVA during preparation can produce highly molecular sieve of SBA-15 with thick pore and high hydrothermal stability. The result of the specific surface area by the adjunct of PVA is 687 m^2/g. The role of PVA serves as a mild template to

produce better structural properties [9]. Therefore, one of the most significant currents investigates the effect of the amount PVA to explore the significantly high surface area, hydrothermal stability, and morphology of silica SBA-15

The methodological approach taken in this study is a combination of the amount of PVA and time adjusting for hydrothermal treatment. One of the most significant current studies in control of the pore size and mesoporous structure of the material is modified process variable during the preparation of typesetting Pluronik as a surfactant template and interaction process between surfactant and precursor silica source. Part of the purpose of this study was to investigate the modification variable synthesis to affect the physical sorption properties and mesoporous structure of the final product. The product of silica SBA-15 was analyzed by nitrogen physisorption, scanning electron microscopy (SEM) with energy dispersive x-ray analysis (EDX), fourier transformed infrared spectroscopy (FTIR), and x-ray diffraction (XRD)

2 Materials and methods

2.1 Materials

The chemical reagent used to prepare the mesoporous silica SBA-15 were Pluronics (P123, $PEO_{20}PPO_{70}PEO_{20}$, average M_n ~ 5800 Sigma-Aldrich, Singapore), tetraethyl orthosilicate (TEOS, 98% Sigma-Aldrich, Singapore), polyvinyl alcohol (PVA Sigma-Aldrich, Singapore), hydrochloric acid solution (HCl, 37% Merck), ammonium fluoride solution (NH_4F), and heptane solution (C_7H_{16}) were received from J.T. Baker. All chemicals reagent which were analytical grade without further purification.

2.2 Synthesis mesoporous silica SBA-15

SBA-15 was synthesized according to the improved procedure by Liang Chao et.al [4,5,9]. The previous study has assessed the properties of SBA-15 without co-surfactant PVA in the preparation process of Pluronic surfactant template [21]. A case study approach was near modified to synthesize SBA-15. For the first, 2.4 g of Pluronic and 0.027 g of NH4F were mixed in 1.3 M HCl solution as much 84 ml, followed by stirring at ambient temperature until the solution was clear. Then, the water-bath set at a temperature 10°C to prepare the Pluronic surfactant template for 1 h. In other solution, various of the amount PVA (1 g for the SBA_1, SBA_2, and SBA_5; 2 g for SBA_2 and SBA_4) were dissolved in 10 ml H_2O at 60°C and mixed into the Pluronic surfactant template. In particular, 3.7 ml of TEOS precursor solution and 1.2 ml heptane were attached to the beaker. The Pluronic surfactant template and TEOS precursor solution were stirred to allow the solution to mix well for one day at room temperature in an open container. After that, the solution was transferred to the closed-teflon container for hydrothermal treatment at temperature of 100°C) for certain time (20 h for SBA_1 and SBA_2; 24 h for SBA_3 and SBA_4; and 96 h for SBA_5), it was then cooled to room temperature. The white gel products were precipitated by centrifuge to get the right product and washed it with deionized water until pH 7 was clear. Finally, to remove partial washing water, the right products were dried at 60°C for 24 h and calcined in the furnace at 550°C for 5 h to perfect the step process.

Table 1: Summary of synthesis condition for SBA-15 samples.

SBA-15 samples	Time of hydrothermal treatment (h)	Amount of PVA (g)
SBA_1	20	1
SBA_2	20	2
SBA_3	24	1
SBA_4	24	2
SBA_5	96	1

2.3 Characterization

2.3.1 Physisorption analysis

Physisorption analysis of SBA-15 samples were quantified at -196°C by using a Quantachroma NovaWin version 11.0 device. The physisorption analysis was measured after the purge process under vacuum at 300°C for 3 h. The amount of nitrogen adsorbed at a relative pressure $[p/p_o]$ = 0.98 was equivalent to analyzed the total pore volume of SBA-15 samples. The data from BJH pore size distribution desorption is required to determine exactly pore size distribution (PSD). The adsorption-desorption isotherm properties for analyzing specific surface area (S_{BET}) was obtained using the multi-point BET data.

2.3.2 Physicochemical properties

Using the X-ray diffraction (XRD) and verifying at the actual pore structure properties, it was possible to identify the

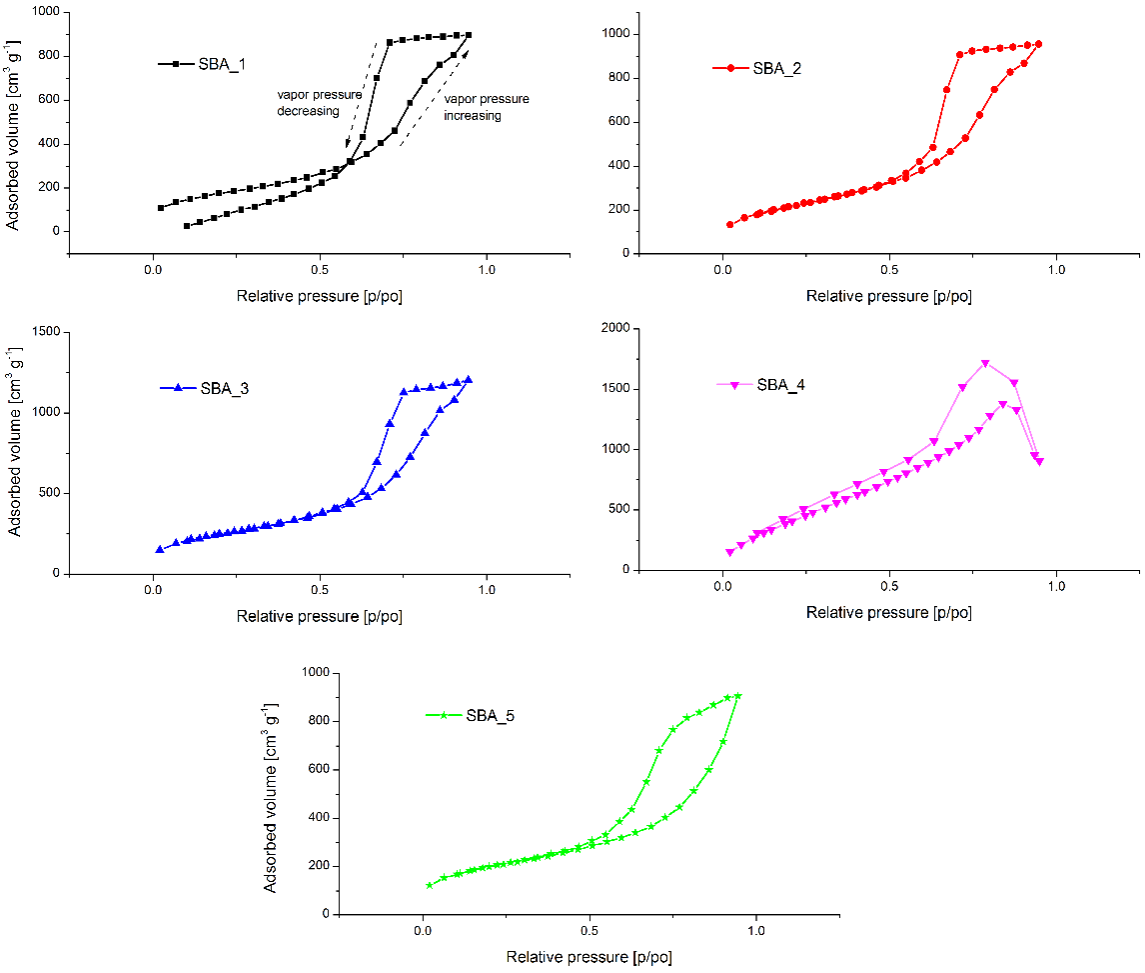

Figure 1: Nitrogen adsorption-desorption isotherm of SBA-15 samples.

crystal phase of SBA-15 samples. The instrument analysis XRD pattern was measured using Bruker D8 Phaser Diffractometer model with Cu kα radiation source with wavelength = 1.5406 Å, kβ 1.3922 Å, and run of the X-ray tube at 40 kV, 20 mA. The diffraction data were observed in the 2θ range from 5° to 90°, with a step size of 0.02° and the step time of 1 s. To analyze the surface morphology and the content of SBA-15 samples were characterized by using a scanning electron microscope (SEM with EDX) SU3500 model, running distance at 4940 µm and 10 kV of electron voltage with the high energy electron beam. The content of Si and O spectrum were determined by SU3500 EDX type at 15 kV and lifetime 30 s. The instrument of 8400S SHIMADZU infrared spectroscopy was used to present data about chemical bond and functional groups of SBA-15 samples base on their characteristic absorption of infrared radiation in vibrational modes. For SBA-15 samples, we used scanned 450-4000 cm^{-1} of the range wavenumbers and ground together with KBr to the made pellet and placed into the DRIFT cell.

Ethical approval: The conducted research is not related to either human or animal use.

3 Result and discussion

3.1 Physisorption isotherm analysis

Surface area is a key property of mesoporous materials by physisorption methods [21]. The result obtained from the preliminary analysis of high surface area for SBA-15 is presented in Figure 1. Interestingly, the increased surface area of SBA-15 at higher *p/po* (0.7-0.9) is related to *Type IV* isotherm [22]. The nitrogen adsorption on samples occur at the beginning process P/Po at the range of 0 to 0.5 was

Table 2: Physisorption analysis of SBA-15 samples with some variables.

SBA-15 sample	Conditions	S_{BET} (m^2/g)	Dp (nm)	Vp (cc/g)
1	PVA 1 g, 20 h	628	4.4	1.40
2	PVA 2 g, 20 h	780	3.8	1.48
3	PVA 1 g, 24 h	892	4.2	1.87
4	PVA 2 g, 24 h	1726	3.2	1.40
5	PVA 1 g, 96 h	699	4.0	1.40

adsorption in microporous initiated with the single layer of the material surface. On relative pressure of 0.6 to 0.9, there was parallel hysteresis loop adsorption-desorption, in which the adsorption of vapor pressure increasing is followed by desorption of vapor pressure decreasing simultaneously. It shows that the sample was mesoporous material and has uniform size pore

Figure 1 presents a typical isotherm, it is a relation of the amount of adsorbed volume and the relative pressure of adsorbed. A feature of the *Type IV* isotherm is typical for porous materials. At higher pressure, there is a hysteresis loop that can explain how the pore is shaped and identified with specific pore structure. All samples show a confirm step with a hysteresis loop corresponding type of H1 with narrow pore size distribution. Figure 1 provides some of the main characteristics of mesoporous materials. It is encouraging to compare this figure with that found by other authors [4–6].

The nitrogen sorption measurement by the Brunauer-Emmett-Teller (BET) method has the most widely used standard for the calculation of the surface area [22]. One unanticipated finding was that the higher surface area of SBA_4 sample of 1726 m^2/g, the pore volume of 1.4 cc/g, and pore diameter of 3.2 nm. There are several possible explanations for this result. Change in the amount of PVA and the time for hydrothermal treatment were compared using physisorption analysis. The interaction of PVA with surfactant template during preparation process indicated that near significant effect on the micelles formed of P123. These results suggest that the diameter and pore volume for all samples are relatively stable. However, the interaction of PVA occurs on the surface area of silica. In the future investigation, it might be possible to use a different condition of time hydrothermal treatment and some variables synthesis of mesoporous materials. The correlation between the time of hydrothermal treatment and the amount of PVA by physisorption analysis is shown in Table 2.

Table 2 presents the experimental data based on the surface analysis (S_{BET}), pore diameter (Dp, nm) and pore volume (Vp, cc/g). The results of the correlational analysis are presented in Table 2, the higher surface area of SBA_4 generated the lower pore diameter. A positive correlation was found between surface area increases and the pore diameter decreases. The pore volume of the samples not significant, only in the range of 1.40 to 1.87 cc/g. The largest pore volume was SBA_3 (PVA 1 g, 24 h), we can see that the amount of PVA did not effect expanding the pore volume. In the current study, comparing the role of PVA only affect to increase surface area, but no interactive with micelles formed from the surfactant template [4]. However, it is different for the time of hydrothermal treatment. The effect of time hydrothermal treatment and the amount PVA on the particle size distribution of mesoporous silica SBA-15 was explored, and the results are presented in Figure 2. The graph shows that there has been stable in pore volume and pore diameter for all the samples

As shown in Figure 2(left), SBA_3 (PVA=2 g, t=24 h) had a surface area of 892 m^2/g and pore volume of 1.87 cc/g. However, if the time of hydrothermal treatment increased the surface area and pore volume is decreased. This condition can be seen at SBA_5 (PVA=2 g, t=96 h). In reviewing the literature, no data was found on the combination between the addition of PVA and adjusting of time hydrothermal treatment. The result of the correlation analysis is summarised in Figure 1. The addition of the amount PVA 2 g and time hydrothermal is raised from 20 h to 96 h, the surface area was increased but the pore volume and pore diameter were slightly more stable. It can be compared to Figure 1 for SBA_1, can be explained that the time of TEOS as a precursor interacts with the surfactant template at the condensation step in teflon has not reached perfect time. Further work, this is an important issue, it requires the higher surface area, the larger pore volume and pore diameter we can do addition PVA 2 g by adjusting the time of hydrothermal treatment in the range 24 to 96 h.

3.2 X-ray diffraction analysis

Powder X-ray diffraction method was applied to characterize the crystal phase and structure of SBA-15 samples. The X-ray diffraction pattern was at 2θ between 5° and 90° for five SBA-15 samples. Figure 3 shows that the SBA-15 has been successfully formed the based on the amorphous peak approach at $2\theta = 23°$, corresponding just to the planar (100) with hexagonal planar symmetry (*p6mm*) [23]. All the samples are amorphous material around 82%.

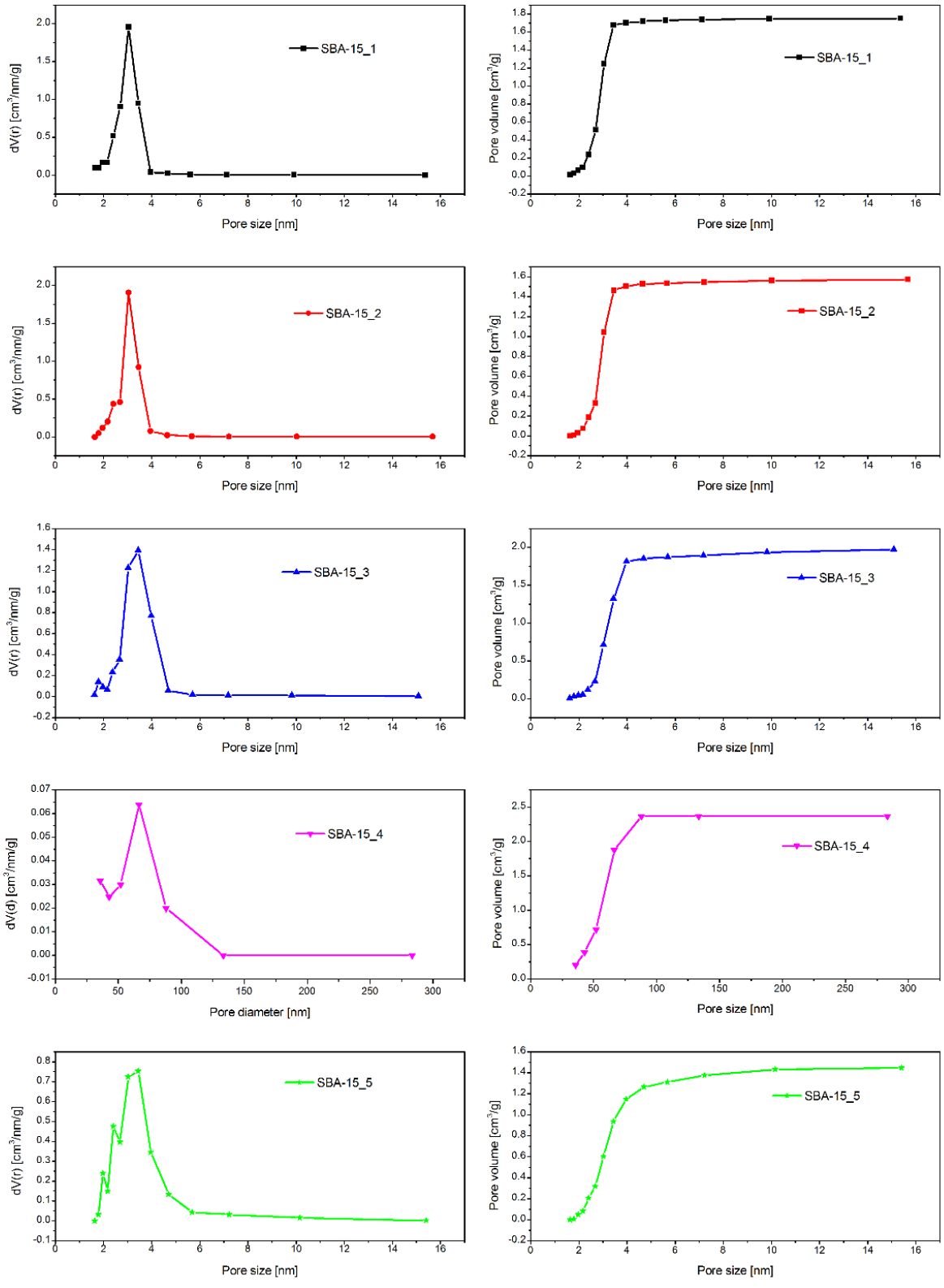

Figure 2: Pore size determination of SBA-15 samples. BJH desorption particle size distribution (left); the relation between pore size and pore volume (right).

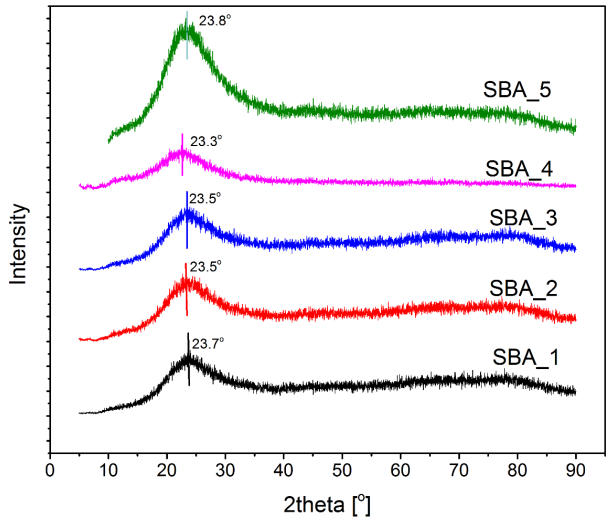

Figure 3: X-ray diffraction pattern on the SBA-15 samples.

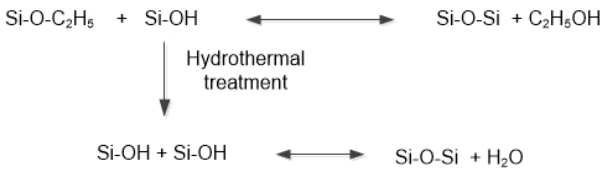

Figure 4: Reaction mechanism of silica.

Except for the sample of SBA_1, it has been investigated that the crystal system is orthorhombic (not general properties of SBA-15) with space group *pmmm*, d spacing of the silica is 20.5 Å corresponding to a unit cell parameter, a_o = 20.57 Å and b_o = 9.74 Å. This case can be explained that the amount of PVA 1 g for 20 h of the time hydrothermal treatment had not been reached to the hexagonal structure of SBA-15. This result diffraction pattern was corresponding to the match with COD-InorgREV204654. Although the exclusion of the crystal structure can reduce the effect of the amount PVA and the time of hydrothermal treatment, these result should be interpreted with caution [3,4]

In one well known recent experiment, limit on wide-angle X-ray diffraction (WAXRD) pattern was found to be diffusion straight peak of amorphous materials at 2θ = 23° was reported [23]. As shown in Figure 3, the peak amorphous of SBA_5 reported significantly more than the other samples. From the data in Figure 3, it is apparent that the length of time for hydrothermal treatment, the amorphous part can be increased. The amorphous part for the sample of SBA-15 were 81.4%; 83.4%; 82.6%; 82.4%, and 83.6% respectively. The value of amorphous composition suggests that a weak correlation may exist between the amount PVA and the time for hydrothermal treatment. A further study with more focus on the amount PVA is therefore suggested.

Figure 5 presents the result obtained from the formation of the surfactant template. The template of mesostructure SBA-15 can be arranged during the preparation process of Pluronic. Micelle formation with Pluronic plays an important role in the structure of mesoporous materials. The critical micelle concentration (CMC) of the surfactant template can do in several varieties of pore size and mesostructure. The influence of addition PVA in the preparation process of mesoporous silica materials has increased the surface area [4]. The next interaction between TEOS as a silica precursor and Pluronic by hydrothermal treatment to high stability materials [9]. Calcination process to remove the surfactant template. The end of the process, silica mesoporous SBA-15 was obtained with high surface area and high thermal stability. Interestingly, the various preparation surfactant template and addition PVA were observed to huge potential application in many industries.

3.3 FTIR spectroscopy analysis

The function group and feature of the SBA-15 samples were identified base on FTIR analysis. The FTIR spectroscopy analysis of SBA-15 has verified that the band absorption of spectra from Si-O, Si-O-Si, Si-OH, and –OH were performed. The spectra of the samples can be compared for vibration peak of the characteristic silica SBA-15. The band absorption peaks from the Figure 4 can be seen 477 cm^{-1}, 817 cm^{-1}, 1215 cm^{-1}, 1641 cm^{-1}, and 3462 cm^{-1} were characteristic peaks IR for SBA-15 materials

Spectra of all samples are shown in Figure 6, that the peaks at 816 cm^{-1} with strong intensity by the presence of SiO-H groups [23]. The bending of the O-Si-O defined near at 478 cm^{-1} with stretching vibration of the existence of silanol groups. The sharp peak at 1646 cm^{-1} indicates that the formed –OH groups (H-O-H) [15,25]. The bands at the peak 3468 cm^{-1} were defined to the band group H-O-H (H_2O molecules) [26]. In fact, the characterization of SBA-15 samples is identified with similar spectra in the mesostructure of the various synthesized of SBA-15.

3.4 Morphology analysis

The scanning electron microscopy (SEM) image of the SBA-15 samples (SBA_3 and SBA_5) is shown in Figure 5

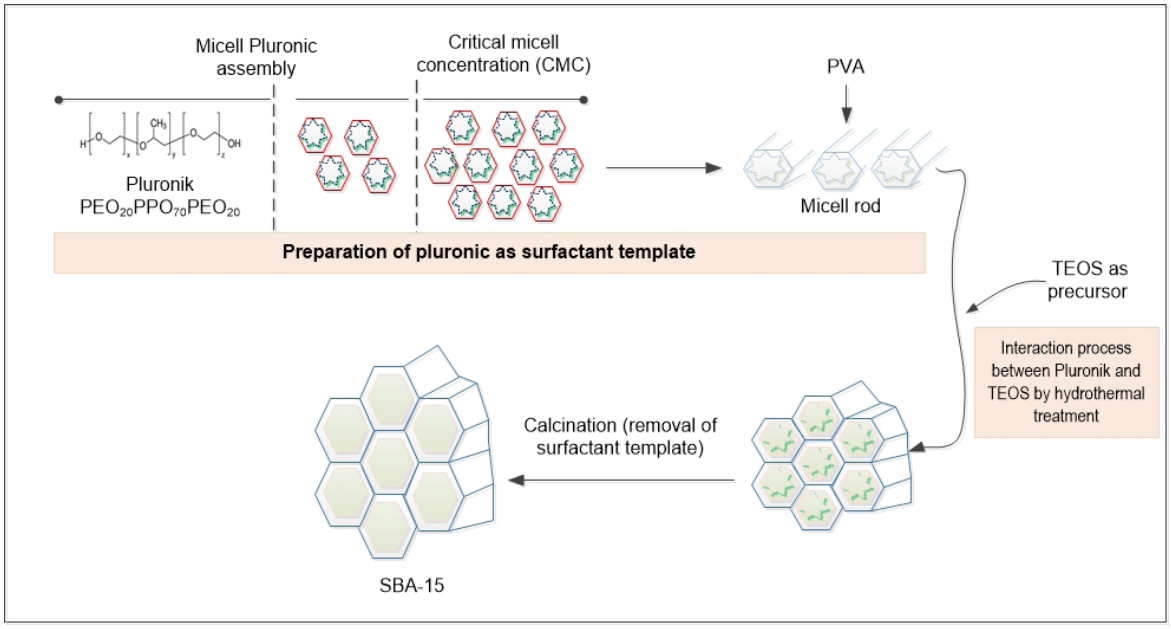

Figure 5: Illustration of the formation mesostructure of SBA-15 [6,24].

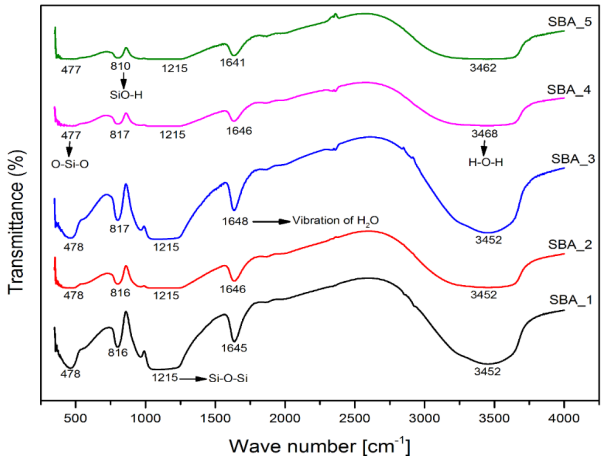

Figure 6: FTIR spectra of the SBA-15 samples.

successively. SEM analysis was incredible analysis for showing the surface morphologies of SBA-15 samples. Figures 5 shows that the mesoporous silica SBA-15 consists of the narrow pore with well ordered hexagonal arrays of mesoporous materials [25,27,28]

The comparison between Figure 7(a) and 7(b) reveals that the increased the time of the hydrothermal treatment can reduce the aggregate into well ordered porous materials. The SEM image of SBA_5 gives an expression that the sample relative uniform. The longer hydrothermal treatment (96 hours) caused the more number of a particle formed with smaller size, it was caused by the interaction

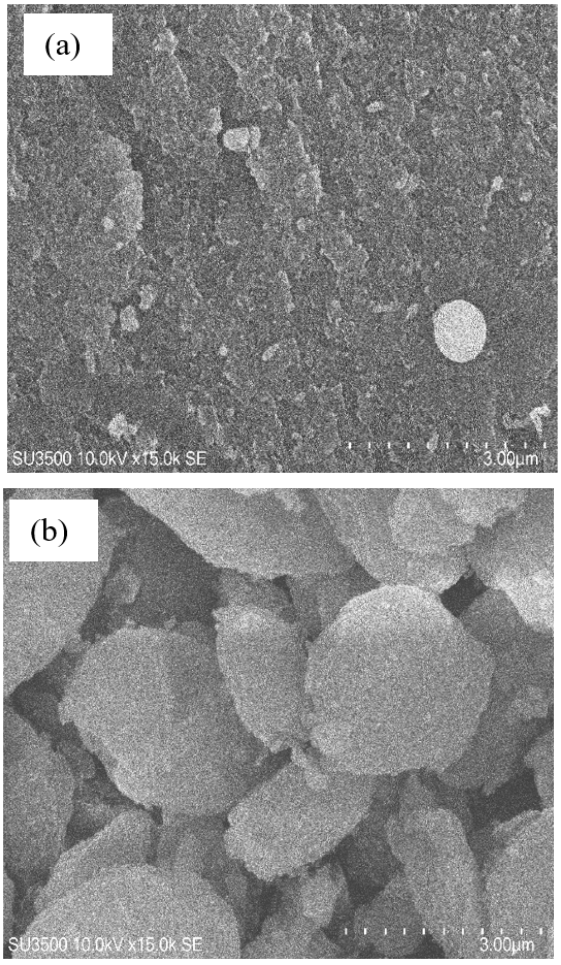

Figure 7: SEM image of the SBA-15 samples: (a) SBA_3 and (b) SBA_5.

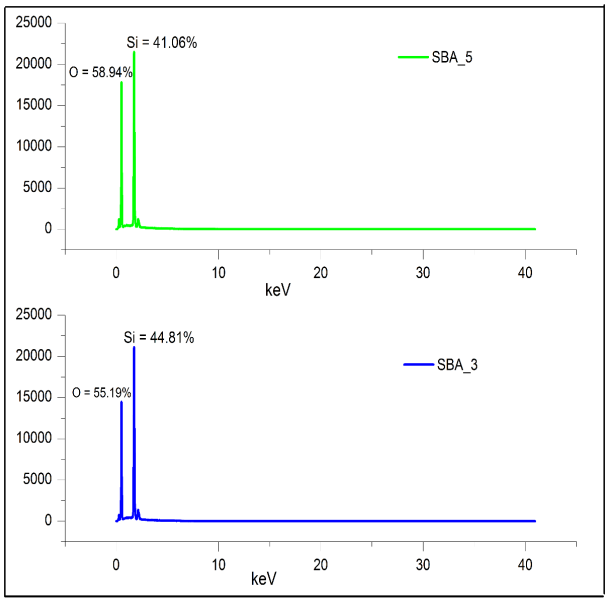

Figure 8: SEM EDX of the SBA-15 samples.

time between micelle surfactant and precursor formation during hydrothermal treatment. The resulting analysis of SEM has same correlation with XRD analysis, in which SBA_5 (amorphous part = 83.6%) has a higher amorphous level compare to SBA_3 (82.6%)

Compositional analysis of surface morphology and topology from SBA-15 is considered by SEM/EDX as shown in Figure 8. The EDX spectra of SBA_3 and SBA_5 indicated the presence of Si = 44.81% and oxygen = 55.19%, for SBA_5 indicated the weight composition of Si = 41.06% and the composition of oxygen are 58.94%. The percentage of silica in the EDX analysis was identified that the synthesized silica material had been successful with uniform composition. This result can be proven by physical-sorption analysis, which the parallel process adsorption by desorption simultaneously

4 Conclusion

The high surface area of SBA-15 was synthesized base on an addition to the amount of PVA and adjusting the time of hydrothermal treatment. Physicochemical properties have been characterized by XRD, FTIR, and SEM/EDX. The BET method was found the higher surface area from the SBA_4 by addition of 2 g PVA and 24 h for the time hydrothermal treatment. The addition of a little amount of PVA and a short time hydrothermal treatment (SBA_1) can be changed to orthorhombic crystal structure and has a lower surface area than all samples. It can be suggested that the silica mesoporous SBA-15 will have potential application prospect in catalysis, storage, and adsorbent

Acknowledgments: Authors would wish to Ministry of Research, Technology and Higher Education of the Republic of Indonesia, for the Doctoral Grand Program in 2018 and Scholarship for Postgraduate Education in the Country for financial assistance to carry out the research.

Conflict of interest: Authors declare no conflict of interest.

References

[1] Ishizaki K, Komarneni S, Nanko (auth.), M. Porous Materials: Process technology and applications, Materials Technology Series 4, 1st ed, Springer US, 1998, ISBN 978-0-412-71110-7.
[2] Sing K.S.W, Reporting physisorption data for gas/solid systems with special reference to the determination of surface area and porosity (Recommendations 1984). Pure Appl. Chem, 1985, 57, 603–619.
[3] Zhao D., Feng J., Huo Q., Melosh N., Fredrickson G.H., Chmelka B.F., Stucky G.D., Triblock copolymer syntheses of mesoporous silica with periodic 50 to 300 angstrom pores. Science, 1998, 279, 548–552.
[4] Zhu, J.; Kailasam, K.; Xie, X.; Schomaecker, R.; Thomas, A. High-Surface-Area SBA-15 with Enhanced Mesopore Connectivity by the Addition of Poly(vinyl alcohol). Chem. Mater. 2011, 23, 2062–2067.
[5] Cao, L.; Kruk, M. Synthesis of large-pore SBA-15 silica from tetramethyl orthosilicate using triisopropylbenzene as micelle expander. Colloids Surf. Physicochem. Eng. Asp. 2010, 357, 91–96.
[6] Johansson, E.M.; Córdoba, J.M.; Odén, M. Synthesis and characterization of large mesoporous silica SBA-15 sheets with ordered accessible 18 nm pores. Mater. Lett. 2009, 63, 2129–2131.
[7] Zhao Dongyuan; Yang Peidong; Melosh Nick; Feng Jianglin; Chmelka Bradley F.; Stucky Galen D. Continuous Mesoporous Silica Films with Highly Ordered Large Pore Structures. Adv. Mater. 1999, 10, 1380–1385.
[8] Norhasyimi Rahmat; Ahmad Zuhairi Abdullah; Abdul Rahman Mohamed A Review: Mesoporous Santa Barbara Amorphous-15, Types, Synthesis and Its Applications towards Biorefinery Production. Am. J. Appl. Sci. 7, 1579–1586.
[9] Wang, J.; Ge, H.; Bao, W. Synthesis and characteristics of SBA-15 with thick pore wall and high hydrothermal stability. Mater. Lett. 2015, 145, 312–315.
[10] Rahmat, N.; Abdullah, A.Z.; Mohamed, A.R. A Review: Mesoporous Santa Barbara Amorphous-15, Types, Synthesis and Its Applications towards Biorefinery Production. Am. J. Appl. Sci. 2010, 7, 1579–1586.
[11] Martins, A.R.; Cunha, I.T.; Oliveira, A.A.S.; Moura, F.C.C. Highly ordered spherical SBA-15 catalysts for the removal of contaminants from the oil industry. Chem. Eng. J. 2017, 318, 189–196.

[12] Acosta-Silva, Y.J.; Nava, R.; Hernández-Morales, V.; Macías-Sánchez, S.A.; Gómez-Herrera, M.L.; Pawelec, B. Methylene blue photodegradation over titania-decorated SBA-15. Appl. Catal. B Environ. 2011, 110, 108–117.
[13] Gómez, G.; Botas, J.Á.; Serrano, D.P.; Pizarro, P. Hydrogen production by methane decomposition over pure silica SBA-15 materials. Catal. Today 2016, 277, Part 1, 152–160.
[14] Martins, A.R.; Cunha, I.T.; Oliveira, A.A.S.; Moura, F.C.C. Highly ordered spherical SBA-15 catalysts for the removal of contaminants from the oil industry. Chem. Eng. J. 2017, 318, 189–196.
[15] Chaudhuri, H.; Dash, S.; Sarkar, A. Synthesis and use of SBA-15 adsorbent for dye-loaded wastewater treatment. J. Environ. Chem. Eng. 2015, 3, 2866–2874.
[16] Lashgari, N.; Badiei, A.; Ziarani, G.M. A novel functionalized nanoporous SBA-15 as a selective fluorescent sensor for the detection of multianalytes (Fe3+ and Cr2O72-) in water. J. Phys. Chem. Solids.
[17] Lei, B.; Wang, L.; Zhang, H.; Liu, Y.; Dong, H.; Zheng, M.; Zhou, X. Luminescent carbon dots assembled SBA-15 and its oxygen sensing properties. Sens. Actuators B Chem. 2016, 230, 101–108.
[18] Tomer, V.K.; Devi, S.; Malik, R.; Nehra, S.P.; Duhan, S. Fast response with high performance humidity sensing of Ag–SnO2/SBA-15 nanohybrid sensors. Microporous Mesoporous Mater. 2016, 219, 240–248.
[19] Araújo, M.M.; Silva, L.K.R.; Sczancoski, J.C.; Orlandi, M.O.; Longo, E.; Santos, A.G.D.; Sá, J.L.S.; Santos, R.S.; Luz Jr., G.E.; Cavalcante, L.S. Anatase TiO2 nanocrystals anchored at inside of SBA-15 mesopores and their optical behavior. Appl. Surf. Sci. 2016, 389, 1137–1147.
[20] Ahmed, K.; Rehman, F.; Pires, C.T.G.V.M.T.; Rahim, A.; Santos, A.L.; Airoldi, C. Aluminum doped mesoporous silica SBA-15 for the removal of remazol yellow dye from water. Microporous Mesoporous Mater. 2016, 236, 167–175.
[21] Thahir, R.; W. Wahab, A.; L. Nafie, N.; Raya, I. Synthesis of mesoporous silica SBA-15 through surfactant set-up and hydrothermal process. *Rasayan J. Chem*. 2019, 12, 1117–1126.
[22] Storck, S.; Bretinger, H.; Maier, W.F. Characterization of micro- and mesoporous solids by physisorption methods and pore-size analysis. Appl. Catal. Gen. 1998, 174, 137–146.
[23] Brunauer, S.; Deming, L.S.; Deming, W.E.; Teller, E. On a Theory of the van der Waals Adsorption of Gases Available online: https://pubs.acs.org/doi/abs/10.1021/ja01864a025 (accessed on Aug 16, 2018).
[24] Morsi, R.E.; Mohamed, R.S. Nanostructured mesoporous silica: influence of the preparation conditions on the physical-surface properties for efficient organic dye uptake. R. Soc. Open Sci. 2018, 5, 172021.
[25] Kumar, S.; Malik, M.M.; Purohit, R. Synthesis Methods of Mesoporous Silica Materials. Mater. Today Proc. 2017, 4, 350–357.
[26] Santos, S.M.L.; Cecilia, J.A.; Vilarrasa-García, E.; Silva Junior, I.J.; Rodríguez-Castellón, E.; Azevedo, D.C.S. The effect of structure modifying agents in the SBA-15 for its application in the biomolecules adsorption. Microporous Mesoporous Mater. 2016, 232, 53–64.
[27] Qin, P.; Yang, Y.; Zhang, X.; Niu, J.; Yang, H.; Tian, S.; Zhu, J.; Lu, M. Highly Efficient, Rapid, and Simultaneous Removal of Cationic Dyes from Aqueous Solution Using Monodispersed Mesoporous Silica Nanoparticles as the Adsorbent. Nanomaterials 2017, 8.
[28] Sabri, A.A.; Albayati, T.M.; Alazawi, R.A. Synthesis of ordered mesoporous SBA-15 and its adsorption of methylene blue. Korean J. Chem. Eng. 2015, 32, 1835–1841.
[29] Meléndez-Ortiz, H.I.; Puente-Urbina, B.; Castruita-de Leon, G.; Mata-Padilla, J.M.; García-Uriostegui, L. Synthesis of spherical SBA-15 mesoporous silica. Influence of reaction conditions on the structural order and stability. Ceram. Int. 2016, 42, 7564–7570.